Eur Radiol (2002) 12:2866–2882
DOI 10.1007/s00330-002-1428-9



**W. R. Nitz**

# Fast and ultrafast non-echo-planar MR imaging techniques

Received: 21 August 2001
Revised: 21 February 2002
Accepted: 25 February 2002
Published online: 28 June 2002


W.R. Nitz (✉)
MR Division, Siemens AG,
Karl-Schall Strasse 6,
91052 Erlangen, Germany
e-mail: wolfgang.nitz@siemens.com
Tel.: +49-9131-844482
Fax: +49-913184-3083

W.R. Nitz
Department of Radiology,
University Hospital of Regensburg,
Franz-Josef-Strauss Allee 11,
93042 Regensburg, Germany

**Abstract** The topic fast and ultrafast MR imaging commonly includes relatively slow gradient-echo techniques with spoiled transverse magnetization (FLASH, FFE-T1, SPGR), gradient-echo techniques with partially refocused transverse magnetization (FISP, FFE, GRASS), gradient-echo techniques with fully refocused transverse magnetization (trueFISP, balanced FFE, FIESTA), the multi-echo spin-echo techniques (RARE, TSE, FSE), a mixture of multi-echo spin-echo and gradient-echo techniques (GRASE, TGSE), and finally single-shot techniques (HASTE, SS-FSE, EPI). This article gives a description of the sequence structures of non-echo-planar fast imaging techniques and a list of potential clinical applications. Recent advances in faster imaging which are not sequence related, such as simultaneous acquisitions of spatial harmonics (SMASH) and sensitivity encoding (SENSE) for fast MRI, are mentioned as well as some novel techniques such as QUEST and BURST. Due to the recent success with gradient-echo techniques with fully refocused transverse magnetization (trueFISP, balanced FFE, FIESTA), this "faster" gradient-echo technique is discussed in more detail followed by multi-echo spin-echo techniques that present the counterpart to the multi-echo gradient-echo (EPI) technique, which is not discussed in this paper. Three major areas appear to be the domain for EPI: diffusion; perfusion; and blood oxygenation level dependent imaging (BOLD, fMRI). For all other applications there is ample room for utilizing other fast and ultrafast imaging techniques, due to some intrinsic problems with EPI.

**Keywords** MR imaging · MR angiography · Cine MR imaging · Nuclear magnetic resonance

## Introduction

The imaging potential of MR imaging continues to evolve. In 1973 Lauterbur demonstrated a technique to create a two-dimensional map of the density of nuclear spins [1], and since then a continuous effort for faster acquisition methods has led to a variety of fast and ultrafast imaging techniques. As early as 1977 Mansfield presented his concept of echo-planar imaging (EPI) [2]. He proposed a method which would produce an image in milliseconds, whereas imaging times at that time were typically of the order of 1 h. Other imaging techniques have been introduced in the meantime with the similar goal of reducing measurement time and those techniques named non-EPI techniques are discussed in this paper. The short repetition time (TR) low-angle excitation gradient-echo (GRE) technique [3], also called fast low-angle shot (FLASH) [4], is often called a fast imaging technique and has been proven to be of significance for the diagnosis of a variety of pathologic disorders and hemorrhagic lesions, especially in conjunction with contrast agents. But since this technique is a single-echo

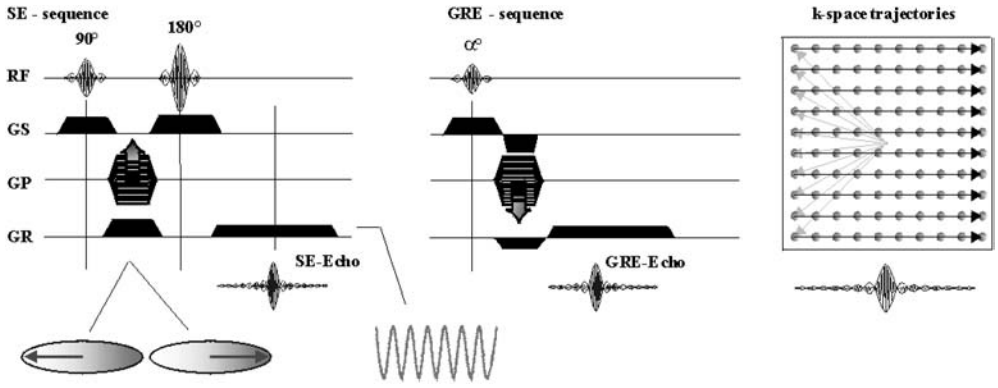


**Fig. 1** The spatial encoding for conventional spin-echo (*SE*) and gradient-echo (*GRE*) sequences. Prior to data sampling, the phase-encoding gradient is applied, establishing a difference in "phase" between the transverse magnetizations within the object, in the direction of phase encoding. A frequency-encoding gradient is switched on during data sampling. Allowing a differentiation between signal sources in the direction of frequency encoding. The data are sorted in a k-space matrix: From top to bottom according to their phase-encoding value, from left to right as frequency encoded in time

method, and not a multi-echo approach as in EPI, it is not the focus of this article.

## History and basic principles

In conventional spin-echo (SE) and GRE imaging a frequency-encoding gradient is switched on during data acquisition causing the resonance frequency being a function of location. The composite signal is later analyzed via a Fourier transformation assigning signal intensities of distinct frequency components to certain locations. For the second dimension, perpendicular to the frequency-encoding gradient, the information about the position of the magnetization vector, the so-called phase, is utilized as source for spatial information. Prior to switching the frequency encoding, a phase-encoding gradient is switched on for a short duration, establishing a difference in phase positions for the magnetization vectors within each voxel in the direction of the magnetic field gradient. In conventional SE and GRE imaging, one line of imaging data (also named one phase-encoding step or one Fourier line or one raw data line or one line in k-space) is collected within each TR period (Fig. 1). The measurement time is then given by the number of phase-encoding steps multiplied by the TR and multiplied by the number of acquisitions (number of averages + 1). In echo-planar imaging (EPI) all necessary Fourier lines are acquired after a single radiofrequency (RF) excitation pulse using multiple gradient echoes, each echo phase encoded (Fig. 2). Main unchallenged applications for EPI sequences are diffusion imaging, perfusion imaging, and functional MRI aiming for the blood oxygenation level dependent (BOLD) effect [5]. There are multiple intrinsic problems to EPI [6], leaving ample room for other fast imaging techniques. As EPI is a multi-echo GRE technique, a non-echo-planar technique should be a multi-echo spin-echo technique such as rapid acquisition with relaxation enhancement (RARE) [7], fast spin echo (FSE) [8] or turbo spin echo (TSE), or a multi-echo mixture of spin echoes and gradient echoes such as gradient-and-spin-echoes (GRASE) [9] or turbo gradient- and spin echoes (TGSE). Recent advances in steady-state free precession imaging (SSFP) demand also the reintroduction of gradient-echo techniques with fully refocused transverse magnetization (FISP [10], true FISP, balanced FFE, FIESTA) as promising non-echo-planar fast imaging techniques. Prior to discussing these sequences, two other recently developed techniques should be mentioned, allowing faster imaging, but not related to any changes in sequence design. As we evaluate the k-space in 3D GRE, we find very low signal amplitudes in the outer Fourier lines containing the information of the high spatial frequencies of the object. The effect is surprising if we omit the measurement of these lines, filling them with zero values instead. The images look better and the measurement time is reduced. This zero-filling approach does not improve spatial or volume resolution but does reduce the artifacts caused by partial-volume effects [11]. The technique applied to a 3D time-of-flight (TOF) magnetic resonance angiography (MRA) is also known as turbo MRA [12] and is illustrated in Fig. 3. The approach is not confined to MRA but can be applied to any 3D technique. A 3D GRE acquisition using this method with a measurement time short enough to hold the breath has been named volumetric interpolated breath hold examination (VIBE) [13]. Figure 4 presents an example of a VIBE acquisition of a hemangioma. As previously mentioned, this technique does not utilize a new sequence, but simply uses a sinc-interpolation via zero filling of Fourier lines, which have never been measured. The other recently introduced methods of faster imaging, which are also not related to a special sequence, are the parallel acquisition techniques such as

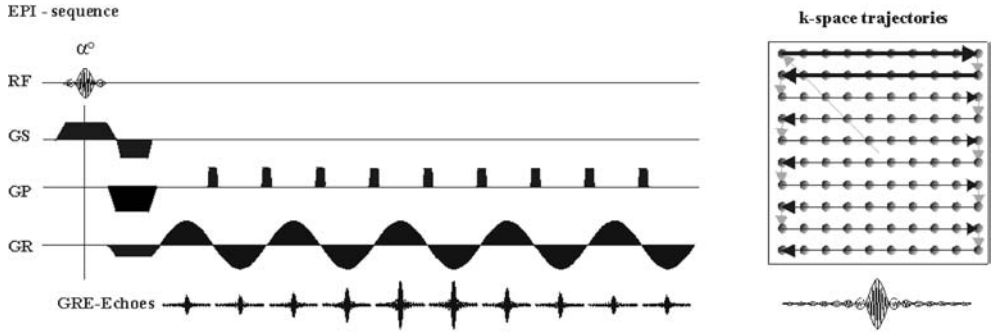


**Fig. 2** One example of a possible echo-planar imaging (EPI) acquisition scheme. The "start position" within k-space is prepared with the preceding gradients in the direction of phase encoding and in the direction of frequency encoding. Advances in phase encoding are provided by gradient "blips" in the direction of phase encoding, in between the bipolar frequency-encoding gradient lobes

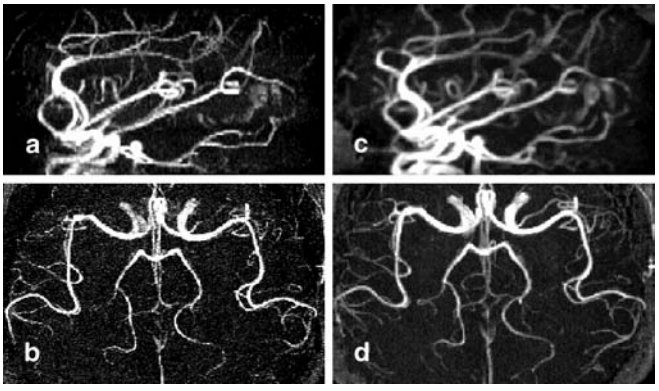


**Fig. 3** **a**, **b** Maximum intensity projections (MIPs) of 12-min duration of measurement of a time-of-flight MR angiography (TOF MRA) acquired on a 1.0-T system. **c**, **d** The MIPs of the same patient during the same session acquired with a "turboMRA" – a study lasting 6 min with interpolation in the direction of depth encoding (zero filling of non-acquired k-space lines)

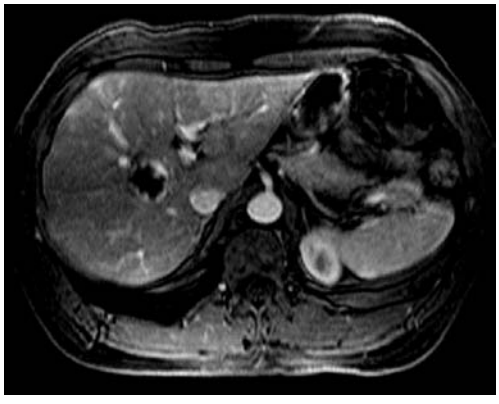

**Fig. 4** Volume-interpolated breath-hold (VIBE) image of a hemangioma after contrast administration. Sequence was of type 3D fast low-angle shot (FLASH) with TR=4.5 ms, TE=2.4 ms, 50 slices (partitions) with a thickness of 2.5 mm (after interpolation), field of view (FOV) 262×350 mm, matrix size 111×256. The circular polarized-body array coil was used in combination with the corresponding coil elements of the spine array coil. A fat saturation pulse was utilized. Measurement time was 20 s, allowing a breath-hold examination

the simultaneous acquisitions of spatial harmonics (SMASH) or the sensitivity encoding for fast MRI (SENSE) [14] methods. Prerequisite for this technique is the utilization of numerous surface or array coils. As each of the surface coils has a specific receiving profile, the signal received from these coils already contains some spatial information – the location of the coil and the sensitivity profile of the coil (Fig. 5). Utilizing this existing spatial information, the number of phase-encoding steps in that direction can be reduced, thus leading to a faster acquisition time.

The intention of this article is to focus on those non-echo-planar fast imaging techniques that have been or are utilized in routine clinical applications. Nevertheless, a few novel approaches shall be mentioned: Using multiple RF pulses, a multitude of spin echoes and stimulated echoes are generated, as pointed out by Hahn [15] as early as 1950. With two exceptions, all sequences disregard the majority of these echoes by spoiling or refocusing them back to the main echo. The two exceptions are a quick echo split NMR imaging technique (QUEST) [16] and BURST imaging [17]. Both methods utilize the various echo paths – each echo getting a proper phase-encoding – and fill the k-space within milliseconds. Although a novel approach, the image quality and resolution achieved so far is no challenge for a conventional sequence. The two successful non-EPI techniques discussed in this article, trueFISP and RARE, also started with inferior image quality as compared with a conventional sequence at the time.

## FISP, trueFISP, FIESTA, SPIDER, projection reconstruction balanced FFE

As mentioned previously, the use of multiple RF pulses during an MR imaging sequence generates a multitude of spin echoes. In techniques such as FLASH [4], those spin echoes or stimulated echoes are spoiled with a spoiler gradient at the end of each Fourier line or the transverse steady state is avoided otherwise by using a random phase position for the low-angle excitation pulse, the so-called RF spoiling [18]. The first sequence

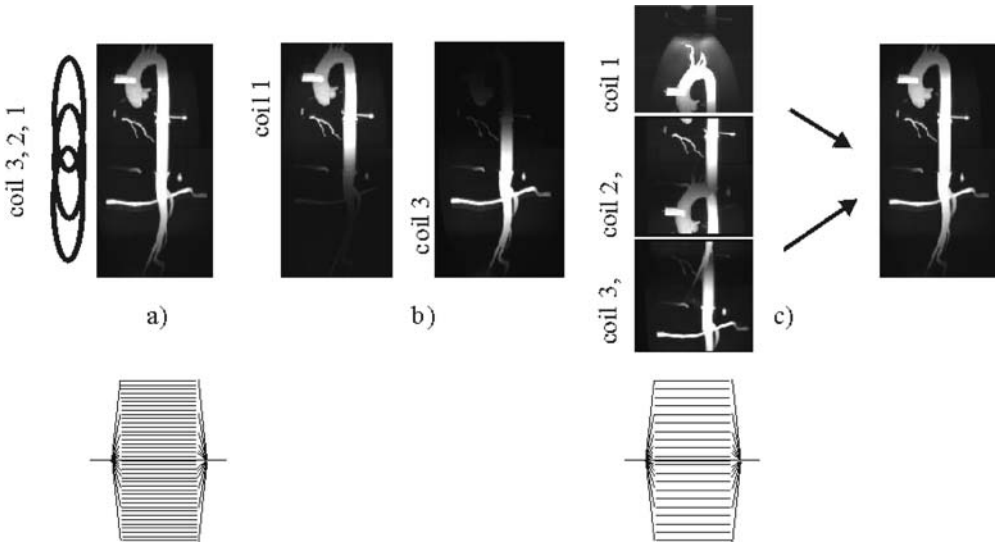


**Fig. 5a–c** Illustration of a "parallel acquisition" technique (sensitivity encoding for fast MRI; simultaneous acquisitions of spatial harmonics) using a vascular phantom. **a, b** The acquisition of a full matrix with **a** all coils or **b** reconstructed separately for each coil. Omitting every second Fourier line will reduce the measurement time by a factor of two, but corresponds to a rectangular FOV. **c** The images reconstructed for each coil will show overfolding artifacts. The appearance of these artifacts depends on the coil positions and the sensitivity profiles of the coils. Using this information, the image can be "unwrapped" (*arrows*)

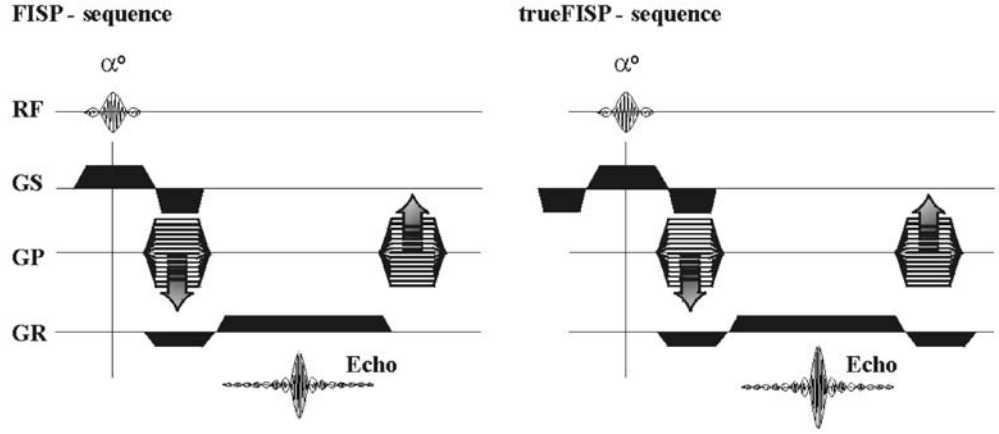


**Fig. 6** Sequence diagram for fast imaging with steady precession (FISP) and trueFISP. For FISP, only the dephasing of the transverse magnetization due to the spatial encoding in the phase-encoding direction is rephased after the data acquisition. In trueFISP, that rephasing is also performed along the frequency encoding and as a preparation also for the expected dephasing during the slice-selection gradient

describing the refocusing of the majority of these echo paths to one main echo was fast imaging with steady precession (FISP) [10], later to be called trueFISP [19]. At the time of the introduction in 1986, gradient systems were not strong enough to allow short TR short TE imaging and the realization of the theoretical benefit of the refocusing. With recent advances in gradient coil and power amplifier technology, the advantage has become more obvious. With short TE and short TR approaches, all tissues with a reasonably long T2-relaxation time will demonstrate additional signal due to the various refocused echo paths (Fig. 6). The FISP is a gradient-echo technique with partially refocused transverse magnetization. Other acronyms for this technique are fast field echo (FFE) and gradient-recalled acquisition in the steady state (GRASS). The trueFISP is a gradient-echo technique with fully refocused transverse magnetization. Other acronyms for this technique are balanced FFE and fast imaging employing steady-state acquisition (FIESTA). The FISP has a history in cardiac applications and trueFISP has the same focus. Compared with trueFISP, the "older" FISP is often used in conjunction with a lower bandwidth, resulting in longer acquisition windows, slightly longer echo times, and, as a consequence, an increased sensitivity to flow- and motion artifacts. The trueFISP is less sensitive to motion due to very short echo times and presents a higher signal intensity due to the additional refocused echo paths (Fig. 7). The only drawback is the sensitivity to off-resonance effects, due to susceptibility gradients within the patient or due to ferromagnetic objects close to the slice to be imaged. In that case, the typical destructive interference pattern (lines of total signal void) can be observed. The trueFISP technique has been combined recently with a so-called radial k-space acquisition scheme. The phase encoding is omitted in this case; instead, two gradients are combined to one frequency-encoding gradient and that gradient is rotated around the imaging plane, similar to the projections in computed tomography. One acronym for this technique is projection reconstruction balanced fast field

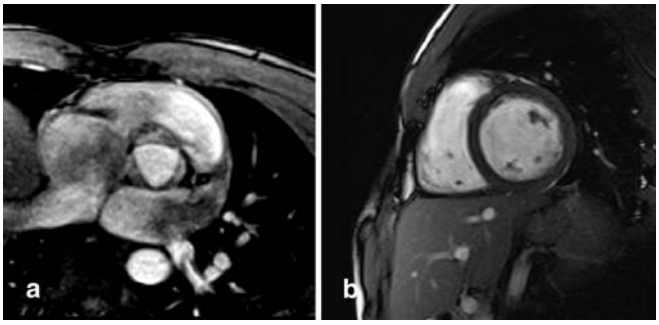


**Fig. 7a, b** Fast imaging with steady precession vs trueFISP. **a** A FISP acquisition through the aortic valve. **b** A short axis representation acquired with a trueFISP technique. The shorter echo time of the trueFISP technique (1.5 vs 2.5 ms) leads to a better edge definition and a reduced sensitivity to flow- and motion artifacts

echo (PR-FFE) [21]. This technique can be further advanced in using multiple gradient-echoes as illustrated in Fig. 8, to fill the k-space even faster. This technique has been named steady-state projection imaging with dynamic echo-train read-out (SPIDER) [20]. Radial acquisition techniques are particularly motion insensitive and seem to be very promising for imaging with a reasonable spatial resolution and high temporal resolution. These techniques show potential for real-time interactive cardiac imaging or fast tracking of interventional devices.

**Fig. 8** Steady-state projection imaging with dynamic echo-train readout (*SPIDER*). The basic sequence structure is of type trueFISP, but there is no phase-encoding gradient. Two gradients are combined to result in a frequency-encoding gradient. For each measurements the gradient amplitudes are varied in order to provide another "projection." The k-space is filled with radial trajectories. Conventional pulse sequences use Cartesian Fourier sampling schemes. Radial k-space acquisitions are usually "regridded" in order to use the same reconstruction algorithm. Three echoes are used within the above example, covering three different projections with one RF excitation

## SINOP and MEDIC

The main difference between GRE imaging and SE imaging is based on the refocusing of the transverse magnetization that has been dephased by mechanisms that are fixed in location and consistent over time. The source for dephasing always originates in a difference in resonance frequencies. As hydrogen nuclei in adipose tissue experience a slightly different electronic environment than the hydrogen nuclei of water molecules, the larmor frequency of adipose tissue is approximately 3.5 ppm lower than the resonance frequency of free water. As a consequence, the transverse magnetization formed by the spin property of hydrogen nuclei of water rotates slightly faster than the transverse magnetization in water-containing tissue. For spin echo that phenomenon is irrelevant, since the faster component gets placed behind the slower component and the transverse magnetizations are, with the exception of the T2 decay, realigned to form the spin echo. For GRE imaging, the magnetization within water speeds ahead as compared with the magnetization within fat, and depending on the selected echo time, both magnetizations will be in phase with each other, opposed phase, or somewhere in between. For the opposed-phase situation, the induced signal may be diminished depending on the water and fat content of the voxel. This appearance can be utilized to identify, for example, adenomas of the adrenal glands [22]. In-phase and opposed-phase images can be acquired simultaneously (Fig. 9) with a double-echo GRE arrangement. Such a technique is also called simultaneous in-phase/opposed-phase acquisition (SINOP).

One of the potential actions to improve the signal-to-noise ratio (SNR) is to increase the number of acquisitions. This approach will automatically increase the measurement time. One interesting method in GRE imaging is to utilize multiple echoes rather than multiple acquisitions. Although the signal diminishes with the echo time,

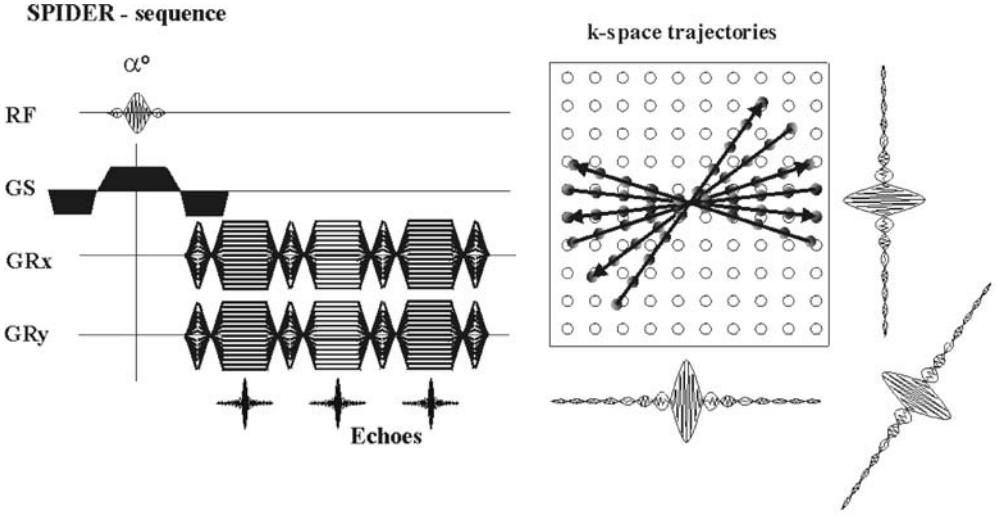

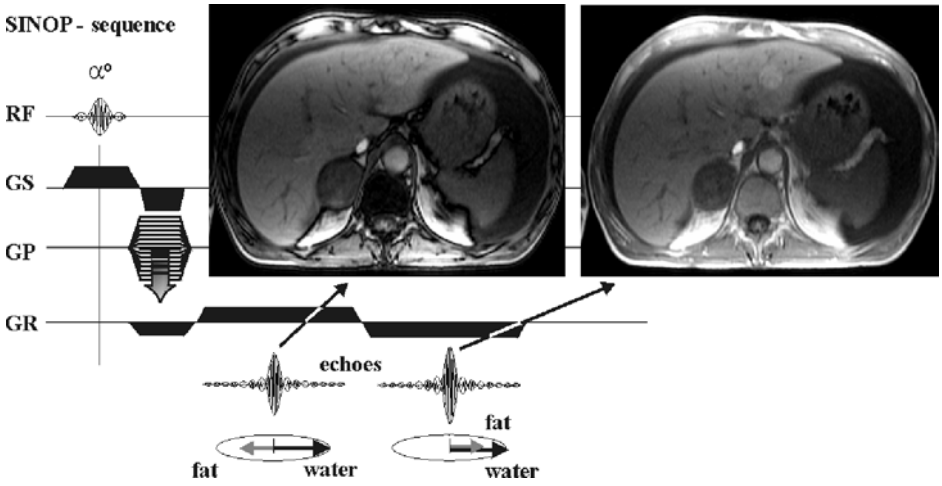


**Fig. 9** Simultaneous acquisition of in-phase/opposed-phase (*SINOP*) images. Depending on the echo time, the transverse magnetization of fat is not aligned with the transverse magnetization of water, leading to signal cancellation within voxel, where the magnetization for fat and water are approximately equal. The above example was acquired on a 1.0-T System (Harmony, Siemens, Erlangen, Germany) with echo times of 3.5 and 7.6 ms, showing an adrenal tumor

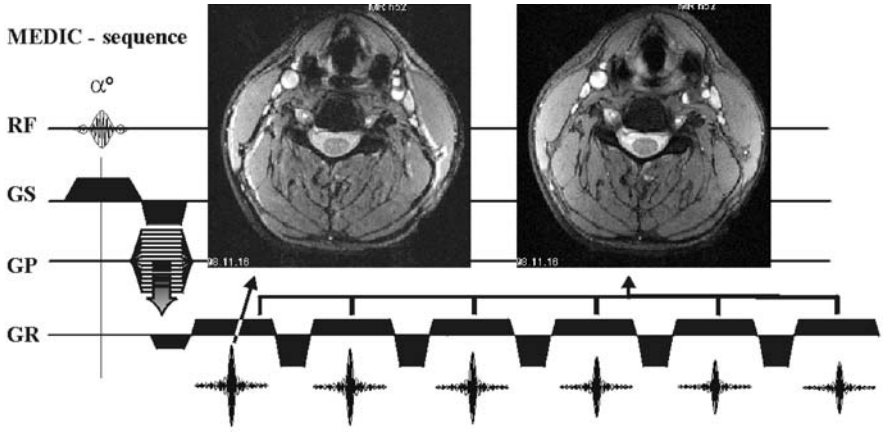


**Fig. 10** Multi-echo data image combination (*MEDIC*). Multiple gradient echoes can be utilized to increase "the number of acquisitions," thus improving signal-to-noise ratio. The T2* decay influencing the later echoes increases the T2*-weighting (effective echo time prolonged)

depending on the T2*-relaxation time of the tissue to be evaluated, if the desired contrast is supposed to be T2-weighted, the method is justified. Such a method has been named multi-echo data image combination (MEDIC; Fig. 10).

## RARE, FSE, and TSE

As EPI uses multiple phase-encoded gradient echoes to fill the k-space, the non-EPI technique doing the same with spin echoes has been named rapid acquisition with relaxation enhancement (RARE) [7]. Instead of collecting one Fourier line per TR, multiple RF refocusing pulses are used to create additional spin echoes and those spin echoes are phase encoded and sorted into the same k-space matrix of the excited slice (Fig. 11). The image quality published at the time was not that impressive. Major vendors were reluctant to include the technique into their products until the rediscovery of multi-echo SE imaging by Melki et al. in 1990, with the finally surviving acronym FSE (fast spin echo) [8]. Other MR equipment vendors, such as Siemens and Philips, implemented a similar method, using the acronym TSE (turbo spin echo) [23]. The potential reduction in measurement time with multi-echo SE imaging is directly proportional to the number of echoes utilized. Usually, the TR is extended compared with conventional SE imaging to achieve a better contrast and to allow time for a multislice acquisition, and usually the matrix size is increased to improve spatial resolution. Both actions eliminate the concern about the consequences of a reduced signal contribution of Fourier lines acquired with late echoes [24]. Figure 12 is a demonstration of an axial T2-weighted brain study acquired within less than 3 min using a TSE imaging technique. As the short TR in GRE imaging allowed the introduction of otherwise too time-consuming volume acquisitions, the same shortening in acquisition time allowed the extension of 3D acquisition techniques towards fast SE imaging [25]. Similar to a 3D GRE data acquisition, a phase-encoding gradient table is introduced in the direction of slice selection, allowing the encoding of the phase position for a 3D slab.

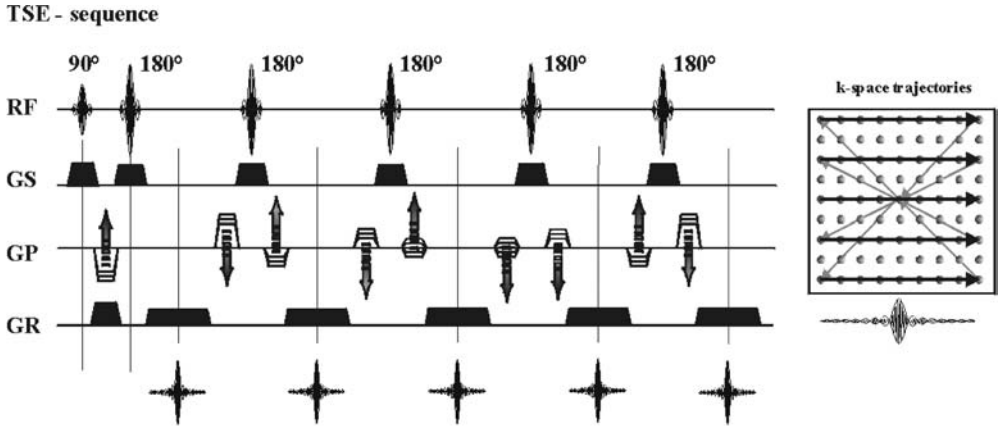


**Fig. 11** Rapid acquisition with relaxation enhancement, turbo spin echo, fast spin echo. The task for filling up a k-space is accelerated by utilizing multiple phase-encoded spin echoes. This example shows five spin echoes. The third echo samples the low k-space frequencies and is named the "effective" echo time. Measurement time is reduced by a factor of five, since five Fourier lines are measured with per excitation

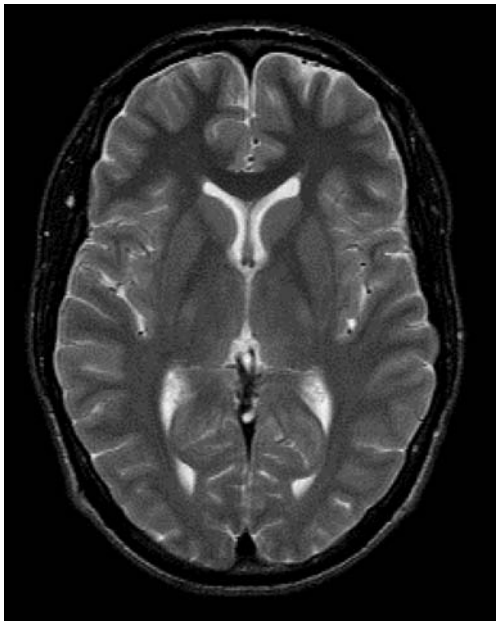

**Fig. 12** Axial T2-weighted image of a normal brain using a TSE sequence. Acquisition time was 2 min 39 s for 19 slices with a slice thickness of 5 mm. Achieved spatial resolution was 0.9×0.4×5 mm. Repetition time was 3790 ms, echo time 98 ms, 11 phase-encoded echoes were utilized per excitation in order to speed up filling of k-space (raw data matrix)

## RESTORE, DRIVE, DEFT-FSE

Another interesting extension of this application is the forced improvement of the longitudinal recovery using a "driven equilibrium pulse" at the end of the echo train, creating a 3D-DEFT-FSE technique [26], also named RESTORE or DRIVE. The driven equilibrium RF pulse at the end of one echo train, sometimes also called restoration pulse, transforms the residual transverse magnetization into a longitudinal magnetization (Fig. 13); the latter leads to an artificial improvement in longitudinal magnetization recovery. Figure 14a shows a sagittal T2-weighted cervical spine acquired with a TSE sequence on a 1.5-T system. Figure 14b shows the same anatomical region and a similar contrast using a TSE sequence with restoration pulse.

One remaining point of concern in comparing fast SE imaging with conventional SE imaging is the reduced sensitivity to susceptibility artifacts, that is the ability to identify hemorrhagic lesions [27].

## TGSE, GRASE

One idea of imaging even faster and at the same time increasing the sensitivity in detecting susceptibility gradients is the combination of spin echoes and gradient echoes (GRASE) [9] also called turbo gradient and spin echoes (TGSE). Instead of collecting one Fourier line after each refocusing RF pulse, multiple gradient echoes are placed inside a spin-echo envelope, each echo phase encoded in order to gather another line with additional spatial information (Fig. 15). The reduction in measurement time is again proportional to the number of refocused spin echoes multiplied by the number of gradient echoes placed under each spin-echo envelope. Unfortunately, the hope for an increased sensitivity in imaging susceptibility gradients has not been fulfilled [28].

## HASTE, SSFSE

An ultimate non-EPI counterpart to a single-shot EPI technique would be a single-shot FSE technique, SSFSE [5]. Such a technique has been introduced and is applied for certain routine clinical applications in combination with the half-Fourier method as introduced by Margosian et al. in 1986 [29]. The technique has been named half-Fourier acquired single-shot turbo spin echo (HASTE) [30]. The half-Fourier method is based on the fact that k-space is symmetrical – at least in theory. A large positive phase-encoding gradient providing a difference of

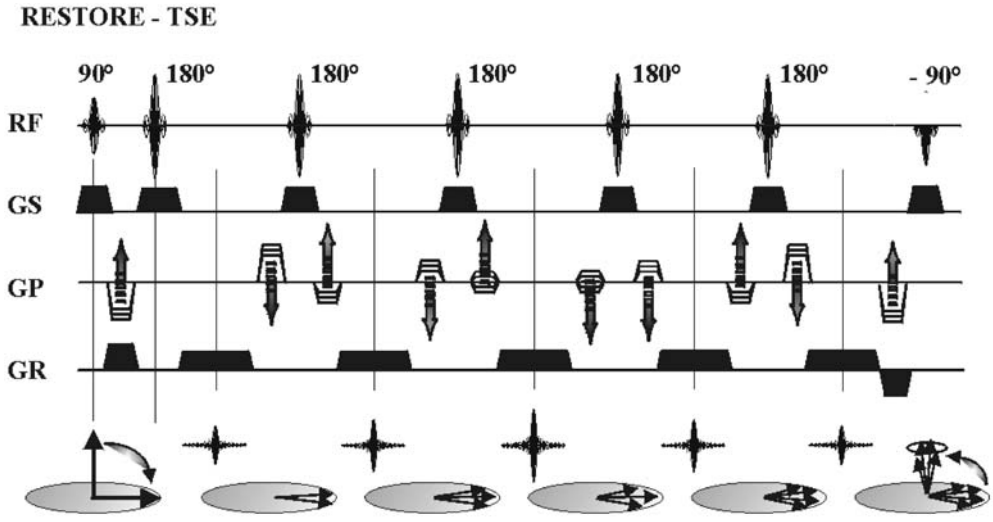


**Fig. 13** RESTORE, DRIVE or DEFT-FSE use a "restoration" pulse at the end of the echo train to convert the remaining transverse magnetization back to a longitudinal magnetization. Tissue with long T2-relaxation times will benefit and will show a larger signal enhancement as compared with a TSE acquisition with similar parameters

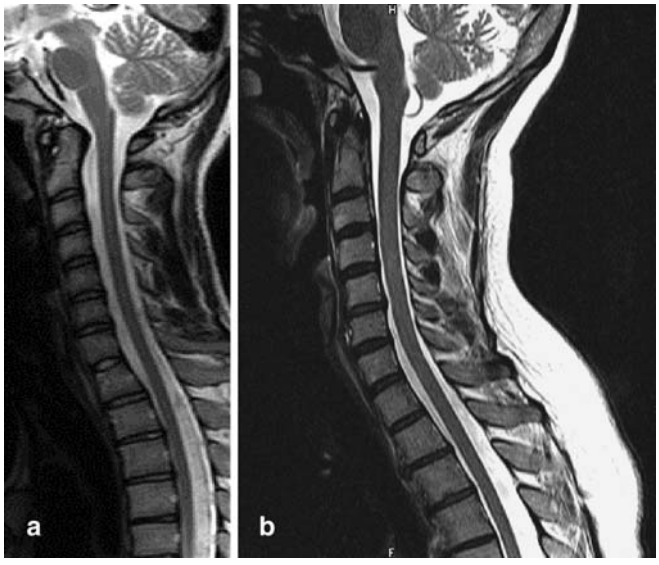


**Fig. 14a, b** Sagittal T2-weighted images of the cervical spine. **a** Image acquired on a 1.5-T system within 4 min using a TSE sequence with a TR of 4 s, an effective TE of 118 ms, and a spatial resolution of 1×1×3 mm. **b** Image acquired on a 1.5-T system within 2.4 min using a TSE sequence with a RF restoration pulse (RESTORE-TSE) using a TR of 4 s, an effective TE of 120 ms, and a spatial resolution of 1.2×0.5×3 mm

180° in-phase positions between the transverse magnetizations of adjacent voxels should provide the same information, the similar signal, as compared with a large negative phase-encoding gradient of the same amplitude and duration. The half-Fourier method therefore measures only half the number of Fourier lines, plus a few to correct the imperfection of the k-space symmetry (Fig. 16).

## Clinical applications

### Brain applications

With the exception of hemorrhagic lesions, FSE imaging or TSE has become part of the routine clinical applications in imaging of the central nervous system, whether it is mass lesions, high-resolution imaging of the pituitary gland, cerebrovascular disease, white matter lesions, intracranial infections, or seizures [31]. The reduction in acquisition time due to the utilization of multiple phase-encoded spin echoes enables high-resolution studies of the brain within reasonable measurement times as demonstrated in Fig. 17. The reduction in acquisition time in FSE imaging made it feasible to introduce inversion recovery techniques with inversion times of the order of 1.8–2.5 s, long enough to null the hyperintense signal of cerebral spinal fluid (CSF) in T2-weighted studies of the central nervous system [32]. The nulling of the signal from CSF is demonstrated in Fig. 18. It was shown that this fast fluid-attenuated inversion recovery (FLAIR), also called turboFLAIR technique, is very sensitive for the evaluation of white matter disease such as multiple sclerosis (MS) [33]. The early and accurate diagnosis of MS has become more important due to the increasing use of immunotherapy in the attempt to modify the course of the disease. Magnetic resonance imaging seems to be sensitive in the evaluation of the response to therapy [34]. TurboFLAIR is also used in the evaluation of subacute and acute hemorrhage. Subarachnoidal hemorrhage is visible as high signal intensity relative to normal CSF and brain parenchyma [35]. Even though turboFLAIR is a T2-weighted technique with dark CSF, the inversion pulse used provides an additional dependency on T1-relaxation time; utilizing the latter, it has been shown that fast FLAIR is superior to contrast-enhanced T1-weighted SE imaging in the evaluation of enhancing meningeal lesions [36].

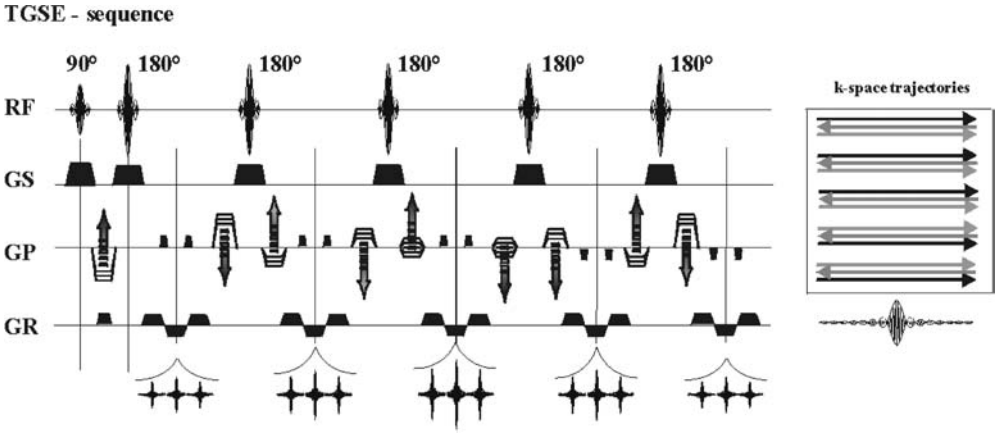


**Fig. 15** A turbo gradient- and spin-echo (*TGSE*) sequence. Acquisition scheme is similar to that of the TSE sequence. Multiple SE envelopes are generated with RF-refocusing pulses. The generated transverse magnetization is phase encoded after each refocusing pulse. In this example, three readout gradient lobes are producing three gradient echoes within one SE envelope. With an additional phase-encoding gradient "blip," the phase can be advanced, allowing the acquisition of another Fourier line per gradient echo. Potential time savings for this setup is of the order of 15 (three gradient echoes times five spin echo envelopes)

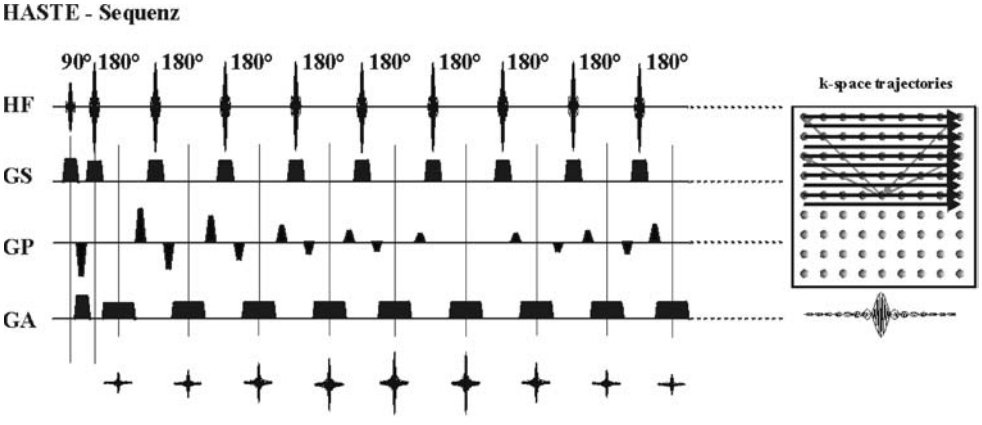


**Fig. 16** A half-Fourier acquired single-shot turbo spin echo (*HASTE*) sequence. Since the k-space is symmetric (in theory), only half of the data is measured using one excitation and multiple phase-encoded spin echoes

## Cardiovascular imaging

The introduction of FSE imaging to study cardiovascular pathology can be seen as a dramatic increase in a diagnostic potential. With FSE imaging it has been possible to generate T2-weighted high-resolution studies of the beating heart, within a single breathhold. The final breakthrough for this application was achieved with the introduction of the "dark blood" preparation scheme [37]. In TSE imaging with dark blood preparation, the measurement of a portion of k-space starts with an inversion of the magnetization of the whole volume, followed by an immediate slice-selective re-inversion. During a delay time of a few hundred milliseconds, the inverted dark blood sitting outside the slice gets washed into the imaging volume and gives no signal for the TSE acquisition part for that portion of k-space. Figure 19 represents a short axis of a heart with pericardial disease, acquired with a TSE imaging sequence with dark blood preparation. The same technique provides a diagnostic tool for the non-invasive exclusion or confirmation of one of the important indications for right ventricular dysplasia [38] – the documentation of fatty replacements in the free right ventricular wall.

For the evaluation of ventricular function, the true-FISP technique generated recent attention due to the increased contrast between the myocardium and the ventricular lumen [39]. That increase in contrast has multiple reasons. The segmented FLASH sequence which has been used in the past for the evaluation of left ventricular function has a relatively long echo time (approximately 6 ms for a bandwidth of 195 Hz/pixel) because it needs a time-consuming three-lobe gradient structure in the direction of slice selection and frequency encoding, in order to rephase the magnetization of flowing structures (gradient motion rephasing, GMR). A long echo time is correlated with a long repetition time and the latter parameter is directly proportional to the measurement time. The trueFISP technique is intrinsically flow insensitive and the refocused echo paths provide enough signal to

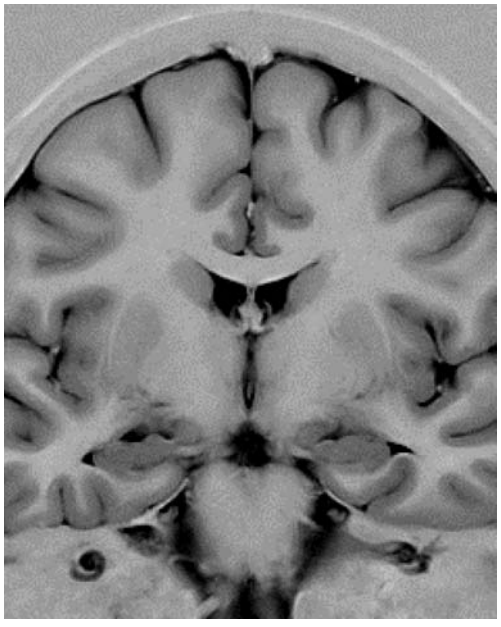

**Fig. 17** Coronal slice through the brain acquired with a turboIR sequence. Similar to the conventional inversion recovery approach an RF inversion pulse is placed prior to the TSE echo train, allowing the enhancement in contrast for small differences in T1-relaxation time. Repetition time was 6.5 s, inversion time 350 ms, and effective echo time 75 ms. Acquisition time was 7 min 43 s for a spatial resolution of 0.3×0.3×5 mm. *GM* gray matter; *WM* white matter; *CSF* cerebral spinal fluid

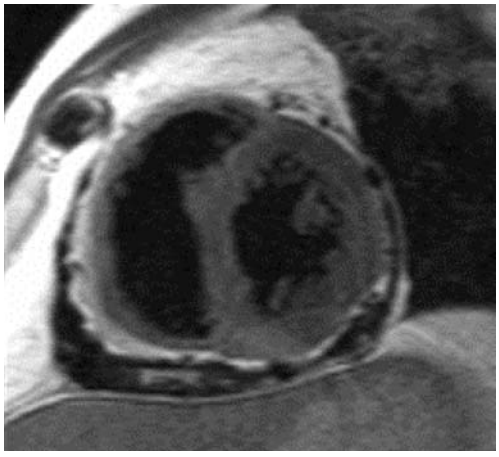

**Fig. 19** T2-weighted short axis view of a heart with thickening of the right ventricular wall. The hypointense asymmetric distribution surrounding the heart is typical for pericardial fluid. The image was acquired with a triggered TSE sequence with "dark blood" preparation. Excitation was repeated every third heartbeat (TR of 2177 ms) followed by 23 refocusing RF pulses generating 23 echoes. Measurement time was 18 heartbeats for a 138×256 matrix

allow the utilization of a higher bandwidth. The omission of the GMR arrangement and the shorter acquisition window of a higher bandwidth provides an echo time as short as 1.6 ms. A short echo time is correlated with a short repetition time. Whereas the segmented FLASH technique allows the measurement of seven Fourier lines per heartbeat, the trueFISP technique allows 15. Figure 20 illustrates one of several views of the beating heart acquired with a trueFISP acquisition scheme. Refinements in trueFISP imaging (mainly shortening the TE and the TR with the help of a strong gradient system and using radial sampling of k-space) enables visualization of the beating heart without any triggering technique [40]. The imaging time of 110 ms for a complete image is fast enough compared with the heart motion, leading

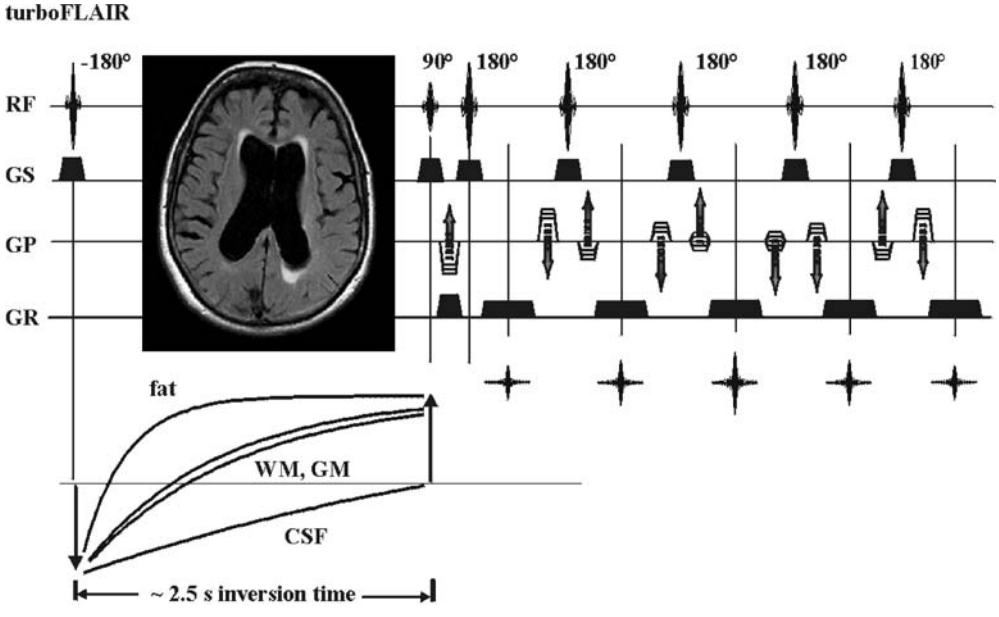


**Fig. 18** Turbo fluid-attenuated inversion recovery sequence illustration and an axial slice of a brain study acquired with this technique that utilizes only the magnitude information. The inversion time was selected long enough to suppress the signal from fluid (1.9–2.5 s). Repetition time was 9.7 s, inversion time 2.5 s, and effective echo time 111 ms. Acquisition time was 1 min 47 s for 15 slices with a spatial resolution of 1×0.8×5 mm. *GM* gray matter; *WM* white matter; *CSF* cerebral spinal fluid

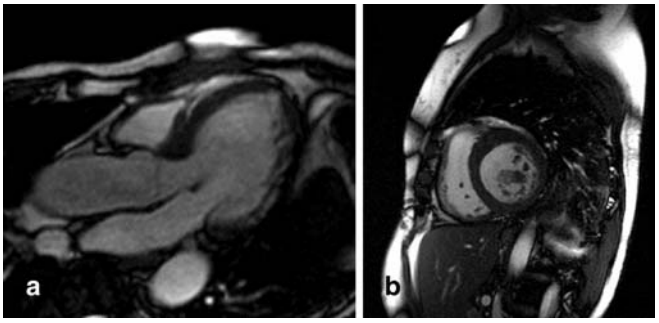


**Fig. 20** **a** Long-axis view of a normal left ventricle showing the open mitral valve during diastole and the closed aortic valve within the aortic outflow tract. **b** Short-axis view of the heart showing a thrombus within the left ventricle. Both images were acquired with a triggered trueFISP technique. Fifteen Fourier lines are measured per heartbeat providing a temporal resolution of 47.4 ms and an acquisition time of ten heart beats for the documentation of heart motion throughout a cardiac cycle. Spatial resolution was 1.8×1.3×6 mm

to an acceptable image quality even for ungated studies – and of course allowing free breathing. The technique shows potential in replacing the slower segmented GRE techniques that were used for the volumetric evaluation of the cardiac ventricles in the course of ischemia, valve malfunctions, congenital abnormalities, cardiomyopathies, pericardial disease, and intracardiac masses. In conjunction with the slow enhancement after administration of gadolinium-containing contrast agents, the trueFISP technique also shows promise to provide complementary information to the perfusion measurements performed with turboFLASH techniques in the evaluation of myocardial viability.

## Abdominal imaging

The utilization of FSE imaging for abdominal imaging is very tempting, since the measurement time can be reduced to the point where breath-hold evaluations will be possible. The image quality of breath-hold examinations vs the image quality of the time-consuming non-breath-hold techniques is simply superior due to the lack of blurring caused by the averaging over the respiratory motion. Numerous investigators have noted that nonsolid liver lesions present a higher signal difference to normal liver parenchyma for FSE imaging as compared with conventional SE imaging; however, this is not the case for solid liver lesions. The lesion conspicuity for solid liver lesions seems to be reduced [41]. The hypothesis is that two mechanisms are responsible for this lower liver to lesion contrast: reduced sensitivity to susceptibility gradients and the altered contrast due to magnetization transfer effects. The lower sensitivity to susceptibility gradients leads to a reduced sensitivity for hemorrhagic lesions [42]. The numerous short-spaced 180° RF refocusing pulses of adjacent slices saturate the invisible water pool of short T2 components [43]. That saturation is transferred to the visible free water via magnetization transfer (MT) mechanisms [44]. Indeed, MT saturation pulses have been used to reduce the signal intensity of solid lesions to distinguish them from hemangiomas and cysts [45]. The hypothesis is that the recovery following MT saturation can be improved with the administration of a gadolinium chelate and may lead to a better conspicuity of solid liver lesions on FSE imaging [46].

The utilization of the half-Fourier technique in conjunction with fast spin echo imaging, also called half-Fourier single-shot TSE technique half-Fourier acquired single-shot turbo spin echo (HASTE) [30] allows a further reduction in measurement. For example, a 128×256 matrix, only 72 Fourier lines are acquired, half the k-space plus a view lines to correct for the asymmetry, leading to a measurement time of 320 ms using an echo spacing of 4.2 ms. The acquisition of those lines follows after a single RF excitation, the reason why this technique is called a single-shot technique. The loss of signal due to the T2 decay, especially for the high spatial frequencies acquired with the late echoes leads to the blurred image appearance of these HASTE images. The major advantage of this technique is the decreased sensitivity to respiratory artifacts, which are still obvious in FSE imaging, since most of the patients are in relatively poor general conditions. It has been reported that for the detection of focal liver lesion HASTE is essentially equal to CT and superior to FSE imaging [47]. Figures 21 and 22 demonstrate the use of T2-weighted breath-hold examinations of the abdomen, using spectral fat saturation in conjunction with a TSE sequence or avoiding the generation of transverse magnetization within fat by combining the short tau inversion recovery (STIR) approach with HASTE.

Fast spin-echo techniques, such as FSE, TSE, RARE and, in conjunction with the half-Fourier method, the single-shot technique HASTE, are especially suited for the visualization of tissues with relatively long T2-relaxation times. This makes them suitable, noninvasive methods for the work-up of patients with pancreaticobiliary disease [48]. The general method is called magnetic resonance cholangiopancreatography (MRCP). Magnetic resonance cholangiopancreatography is a relatively new imaging technique and suggested protocols range from thick single-section TSE imaging (50–100 mm) to thin-collimation multisection TSE or HASTE imaging (3–10 mm). Multisection images are often combined by using maximum intensity projection (MIP) as illustrated in Fig. 23.

Single-shot FSE techniques (SSFSE) have also been used for the evaluation of the colon, i.e., MR colonography [49]. Filling defects within the colon as measured with a 3D GRE technique and a T1-shortening contrast media may point to a mass lesion. Hyperintense signal

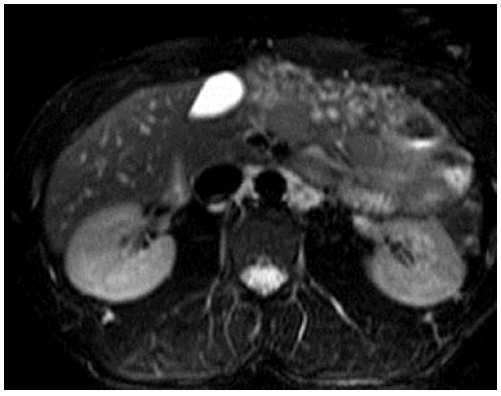

**Fig. 21** T2-weighted abdominal study with spectral fat saturation pulse using a TSE imaging technique with 29 echoes allowing an acquisition time of 16 s for a spatial resolution of 1.9×1.2×8 mm. Repetition time was 4 s, effective echo time 102 ms

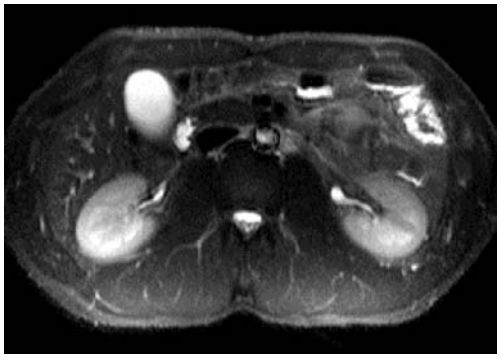

**Fig. 22** T2-weighted abdominal study with relaxation-time-related fat suppression technique acquired with a half-Fourier acquired single-shot turbo spin echo with inversion recovery preparation (HASTE with IR=HIR) after administration of a paramagnetic contrast agent. Acquisition time per slice was 1.2 s. Effective echo time was 57 ms. Inversion time was 150 ms. Spatial resolution was 1.9×1.4×8 mm

within a FSE image at the same location will support that diagnosis [50].

## Genitourinary and gynecologic imaging

The double-echo GRE with simultaneous acquisition of "in-phase" and "opposed-phase" images (SINOP) can be used to differentiate benign from malignant adrenal masses. Contrary to metastases and adenocarcinomas, adrenal adenomas usually show various degrees of fat accumulation. On opposed-phase MR imaging these adenomas show up hypointense as compared to the appearance on the in-phase image. A double-echo acquisition obviates the need for two separate (breath-hold) acquisitions and eliminates potential section misregistration.

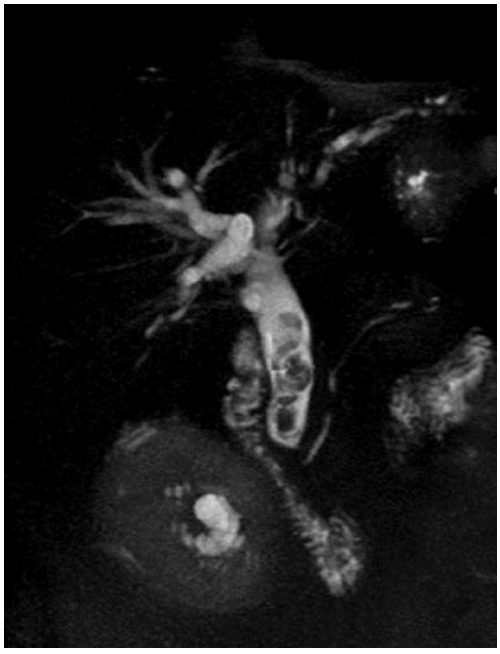

**Fig. 23** A so-called magnetic resonance cholangiopancreatography (MRCP) maximum intensity projection of a heavily T2-weighted coronal HASTE acquisition showing biliary stones and a dilated duct. Effective echo time was 108 ms. Slab thickness was 20 cm. In-plane resolution was 1.1×0.7 mm

The diagnosis of the acute gynecologic condition with MR imaging is based mainly on contrast-enhanced T1-weighted GRE imaging. The rim enhancement in inflammatory lesions is clearly shown and the vascularity of the lesion is documented, and extravasation of contrast material is indicative of bleeding points for hemorrhagic lesions. T2*-weighted images are used for the demonstration of hemorrhagic lesions via the susceptibility artifacts created by deoxyhemoglobin and hemosiderin and air bubbles in abscesses are identified via the correlated susceptibility gradient. Fast spin-echo imaging becomes important for the evaluation of pyosalpinx or abscesses, the latter appearing hypointense to urine because of the presence of hemorrhage or debris. Fast spin-echo imaging with a long effective echo time (250–350 ms) is helpful in all anatomic regions and pathologic conditions, where a simple fluid is to be differentiated from fat or complex fluids [51]. Figure 24 demonstrates a T2-weighted study of a uterus carcinoma acquired with a TSE sequence. Magnetic resonance imaging has become indispensable for accurate staging of gynecologic cancer and FSE imaging has become an integral part of the commonly used protocols [52]. It has been shown that the sensitivity of MR in staging advanced malignancies is superior to CT and Doppler US [53].

**Fig. 24** T2-weighted sagittal study of a uterus carcinoma, acquired with a TSE sequence within 3 min 39 s. Repetition time was 4.1 s, effective echo time 95 ms, and the spatial resolution was 0.76×0.68×6 mm

## Obstetric imaging

Prenatal MR imaging has become popular with the development of fast MR imaging techniques such as the single-shot FSE sequence. Although prenatal MRI has been sporadically used in the past, usefulness has been limited by fetal motion. Maternal or fetal sedation was frequently needed and even the introduction of FSE imaging did not provide the image quality needed for a reliable diagnosis. With the introduction of the single-shot FSE technique, T2-weighted images of the fetus are obtained in less than 1 s per section without significant image degradation by fetal motion. Although ultrasonography remains the imaging technique of choice for prenatal assessment of normal or abnormal fetal development, MR imaging plays an important complimentary role to US due to its excellent tissue contrast [54]. Figure 25 illustrates fetal studies acquired with fast spin echo techniques such as TSE or HASTE [55].

## Musculoskeletal imaging

Magnetic resonance imaging is highly sensitive in the evaluation of discovertebral diseases [56]. Lesions are characterized based on location and signal intensities on T1-weighted images with and without contrast enhancement and on T2-weighted images. Most institutions solely use fast spin echo imaging techniques for T2-weighted studies, due to the better contrast and the higher spatial resolution in a shorter measurement time as compared with conventional SE imaging. A further improvement in T2-weighted imaging of the spine seems to be the utilization of a driven equilibrium RF pulse, allowing T2-weighted 3D imaging of the cervical spine with a repetition time as short as 211 ms within an acquisition time of 4 min 14 s [26]. As T2-weighted imaging has also been used in the past to study the integrity of joints, fast spin echo imaging has replaced the conventional SE protocols for the evaluation of ligamental injuries, documenting joint effusion, edema, or hemarthrosis as hyperintense signal regions on T2-weighted TSE images [57]. Both FLASH and FISP have been used for the evaluation of human articular cartilage [58]; however, for chondral abnormalities as a result of traumatic injury or arthritis the contrast between cartilage and joint fluid is

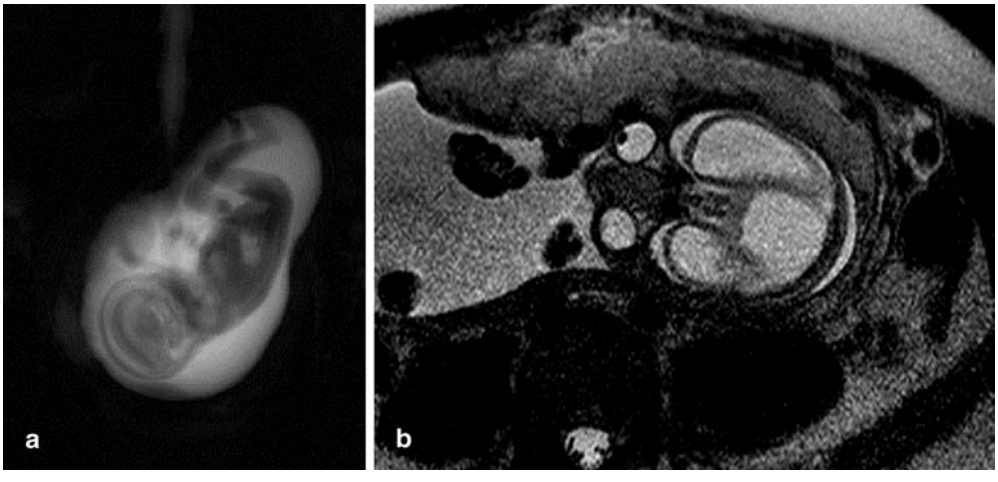


**Fig. 25a, b** Fetal imaging with TSE and HASTE. **a** Image acquired with a TSE technique with an effective echo time of 940 ms. **b** Image acquired with a HASTE sequence (1.85 s per slice) with an effective echo time of 94 ms and a spatial resolution of 1×0.8×3 mm. The hyperintense distribution within the fetal brain is typical for the appearance of cerebrospinal fluid in the case of ventriculomegaly

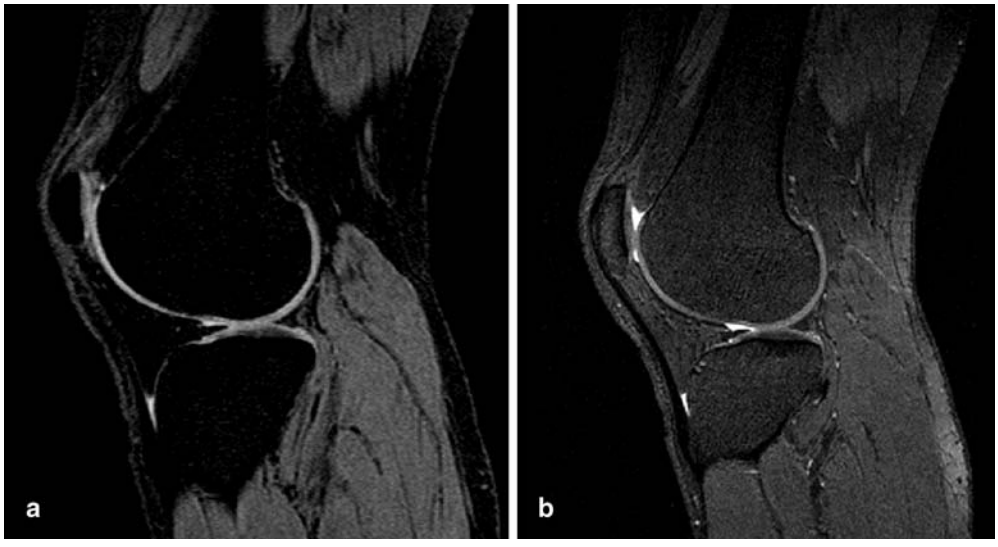


**Fig. 26** **a** This knee study was acquired with a sequence of type FISP with a spectral fat saturation pulse. Acquisition time was 7 min 17 s with a repetition time of 36 ms, an excitation angle of 40°, an echo time of 10 ms, and a spatial resolution of 0.8×0.6×1.5 mm. **b** Image acquired with a sequence of type dual echo steady state (DESS) with water excitation pulse. Acquisition time was 5 min 46 s with a repetition time of 19 ms, an excitation angle of 30°, an echo time of 5 ms, and a spatial resolution of 0.7×0.7×1 mm. This comparison presents the additional T2-contribution of the (S–) component causing hyperintense signal from fluids

frequently inadequate. It remains a matter of opinion whether to consider the dual-echo steady-state (DESS) already a conventional imaging technique or still a fast imaging technique. The DESS technique belongs to the family of steady-state sequences as does trueFISP, and its main advantage is the differentiation between fluid and cartilage. Whereas the trueFISP uses the refocused gradient-echo (S+) and echoes that are generated with the succeeding RF pulse (S–) of next excitations, the DESS sequence acquires the two signals in adjacent acquisition windows and combines the two images [59]. Whereas the (S+) signal has a mixed T1- and T2-weighting, the (S–) component is heavily T2-weighted and significantly increases the signal for fluid. Figure 26 demonstrates the gain in signal by comparing a knee study acquired with a FISP acquisition as compared with a similar study acquired with the DESS technique.

T1-weighted SE pulse sequences remain the most common approach for bone marrow imaging. Exceptions are lesions within areas of red marrow in infants, children, and adults with red marrow hyperplasia. In those cases lesion conspicuity can be increased using a fat-saturated fast spin echo or a fast STIR sequence [60]; the latter, also called turboSTIR, is similar to the conventional STIR. A 180° RF inversion pulse reverses the longitudinal magnetization. Instead of starting a conventional SE acquisition scheme after the short inversion time, the TSE acquisition scheme is initiated. TurboSTIR is also the favorable sequence to identify bone metastases [61]. The main drawback of the turboSTIR sequence is that it does not produce signal from any tissue with a similar T1-relaxation time than that of fat, e.g., blood in hematoma or contrast-enhanced tissue. The fat-free metastases are typically presented as hyperintense signal region surrounded by the low signal of the uninvolved portions of the fat-containing vertebral bodies.

MRI-guided interventional procedures

As radiology is moving from a purely diagnostic institution to a resource that combines diagnosis and therapy, interventions under MR guidance are becoming increasingly important. The main topics where fast non-EPI techniques are playing an increasing role are MR-guided punctures, biopsies, drainages, and tumor ablations. The necessity of a reasonable access to the patient for interventional procedures requires an open-magnet design. Open-magnet designs are usually of low magnetic field strength (0.2–0.5 T). Due to the real-time necessity, the low field is especially challenging, since the lack in SNR is usually compensated with a prolonged measurement time, whereas a sufficient temporal resolution is required for image-guided interventions. The majority of the lesions to be punctured, biopsied, or drained demonstrate a prolonged T2-relaxation time as compared with the surrounding parenchyma. A sequence providing a reliable T2-contrast would be adequate. The trueFISP sequence has been used on low-field systems (0.2 T) for fast (1.4 s/image) T2-weighted imaging of pancreatic cancer, orbital mass, and intradural fluid collection [19]. To achieve a comparable contrast with TSE imaging would have taken 16 s. Another sequence that has been utilized on low-field systems for the visualization of tumors and thermal lesions is PSIF [62]. The sequence name is a consequence of the sequence structure – being a time-reversed version of FISP. The motivation for this sequence results from the fact that FISP and trueFISP are theoretically T1/T2-weighted rather than only T2-weighted, and that they may not always generate a sufficient contrast. A steady-state free precession (SSFP) sequence, such as trueFISP, contains two components: a free induction decay that arises from the most recent RF pulse, the (S+) signal contribution, and a strongly

T2-dependent SE component that forms prior to the upcoming RF pulse, the (S–) signal contribution. The PSIF sequence utilizes solely the heavily T2-weighted (S–) signal contribution and has the potential for fast imaging of lesions with a prolonged T2-relaxation time as compared with the surrounding normal parenchyma.

The mechanisms for temperature mapping with MR imaging during tumor ablation are primarily based on changes in T1-relaxation time, diffusion, and changes in water proton resonance frequency [63]. The method of temperature monitoring based on the phase shift due to change in proton resonance frequency seems to be the preferable choice due to the excellent linearity to the temperature change and the near-independence with respect to tissue type. Relatively "slow (update rate 10 s/image)" GRE techniques have been utilized for the MR temperature mapping [64]. Thermal lesions have been shown to appear as hypointense regions surrounded by a bright rim on T2-weighted images [65]. It has been reported that the hypointense lesion remains visible beyond the return of tissue temperature to normal body temperature which supports the hypothesis that it is an effect of persistent tissue dehydration resulting in a local decrease of proton density and an increase of irrotational water molecule bonds due to tissue coagulation necrosis. The "dynamic" alteration of the T2-relaxation time as a consequence of induced heat has been monitored using a "fast (update rate 20 s/image)" TSE technique [66].

### Comparisons with EPI

Echo-planar imaging is very fast and sensitive, but single-shot imaging offers a limited spatial resolution and is sensitive to local field inhomogeneities. Echo-planar images with resolution and contrast similar to those of conventional MR images can be obtained by using multishot acquisitions. In areas of the brain with large magnetic susceptibility gradients and in other organs that have relatively short T2 (and T2*) relaxation times, single-shot EPI has shown a poor performance. There are three major areas where EPI is the method of choice despite the intrinsic problems. The bulk motion of the brain hampers the measurement of brain diffusion. The most straightforward method to eliminate the effect of motion is to use single-shot diffusion-weighted EPI. The second area is the measurement of brain perfusion. Conventional SE and GRE techniques are not fast enough to capture the first-pass transit of contrast agent from multiple sections in the brain, which requires whole-brain imaging with a temporal resolution of 1–2 s. The third area for EPI is the evaluation of cortical activation or functional MRI where the sensitivity to local field inhomogeneities turns into an advantage for monitoring the oxygenation level of the blood (blood oxygenation level dependent, BOLD).

Diffusion imaging is routinely used for the evaluation of early cerebral ischemia and stroke. Two non-echo-planar techniques have been applied for the measurement of diffusion; one is a modified FSE approach called single-shot diffusion-weighted RARE [67], and the potential of steady-state free precession (SSFP) methods [68], such as trueFISP or PSIF for diffusion-weighted measurements, was realized early. The acquisition of diffusion-weighted images with full sensitivity with RARE requires carefully chosen coherence pathways [69]. The SSFP techniques use the sum of different echo pathways, and hence the diffusion time is poorly defined.

The two main concepts for measuring perfusion are the first-pass tracing of a contrast agent and the labeling of arterial blood (arterial spin labeling, ASL) [70]. For the first-pass approach, EPI is the only method to acquire multiple sections of the whole brain while capturing the passing contrast bolus. Since the spin-labeling technique, the tagging of blood, does not have the time constraints of a passing bolus, a slower technique, such as a modified FLASH technique, can be used for perfusion measurements [71].

The commonly observed alterations in blood oxygenation (BOLD) effect rely on the fact that the increase in blood flow by far exceeds the physiologic oxygen demand. Deoxyhemoglobin is paramagnetic, whereas oxyhemoglobin demonstrates diamagnetic properties. Changes in deoxyhemoglobin levels result in changes in microscopic susceptibility effects and are measured as small increases in image intensity with an imaging sequence sensitive to susceptibility gradients. Most MR functional imaging methods use EPI due to the ability of covering multisections of the brain within 1 s. Fewer researchers have been utilizing a FLASH [72] or echo-shifted FLASH approach [73].

## Conclusion

Echo-planar imaging is unsurpassed with respect to the speed of acquisition and has three major areas where it is the method of choice. Those three areas are diffusion, perfusion, and BOLD imaging. For all other areas there is plenty of room for non-echo-planar fast imaging techniques due the intrinsic limitations of the EPI single-shot technique to achieve a sufficient spatial resolution, a sufficient contrast, and all this without artifacts [6].

**Acknowledgements** I thank S. Danisch and B. Baden for providing the clinical examples, P. Bottomley, M. Deimling, and B. Kiefer for their helpful discussions, and C. Collins for language improvements to this manuscript.

## References


1. Lauterbur PC (1973) Image formation by induced local interaction: examples employing nuclear magnetic resonance. Nature 243:190–191
2. Mansfield P (1977) Multi-planar image formation using NMR spin-echoes. J Phys C 10:L55–L58
3. Edelstein WA, Bottomley PA, Hart HR, Smith LS (1983) Signal, noise and contrast in nuclear magnetic (NMR) imaging. J Comput Assist Tomogr 3:391–401
4. Haase A, Frahm J, Mathaei D, Haenicke W, Merboldt K-D (1986) FLASH imaging. Rapid imaging using low flip-angle pulses. J Magn Reson 67:256–266
5. Poustchi-Amin M, Mirowitz SA, Brown JJ, McKinstry RC, Li T (2001) Principles and applications of echo-planar imaging: a review for the general radiologist. Radiographics 21:767–779
6. Fischer H, Ladebeck R (1998) Echo-planar imaging image artifacts. In: Schmitt F, Stehling MK, Turner R (eds) Echo-planar imaging: theory, technique and application. Springer, Berlin Heidelberg New York
7. Hennig J, Nauerth A, Friedburg H (1986) RARE-imaging: a fast imaging method for clinical MR. J Magn Reson Med 3:823–833
8. Melki PS, Mulkern RV, Panych LP, Jolesz FA (1991) Comparing the FAISE method with conventional dual-echo sequences. J Magn Reson Imaging 1:319–326
9. Oshio K, Feinberg DA (1991) GRASE (gradient- and spin-echo) imaging: a novel fast MRI technique. Magn Reson Med 20:344–349
10. Oppelt A, Graumann R, Barfuss H, Fischer H, Hartl W, Schajor W (1986) FISP: a new fast MRI sequence. Electromedica 54:15–18
11. Du YP, Parker DL, Davis WL, Cao G (1994) Reduction of partial-volume artifacts with zero-filled interpolation in three-dimensional MR angiography. J Magn Reson Imaging 4:733–741
12. Shigematsu Y, Korogi Y, Hirai T, Okuda T, Sugahara T, Liang L, Takahashi M (1999) 3D TOF turbo MR angiography for intracranial arteries: phantom and clinical studies. J Magn Reson Imaging 10:939–944
13. Rofsky NM, Lee VS, Laub G, Pollack MA, Krinsky GA, Thomasson D, Ambrosino MM, Weinreb JC (1999) Abdominal MR imaging with a volumetric interpolated breath-hold examination. Radiology 212:876–884
14. Madore B, Pelc NJ (2001) SMASH and SENSE: experimental and numerical comparisons. Magn Reson Med 45:1103–1111
15. Hahn EL (1950) Spin echoes. Phys Rev 80:580
16. Heid O, Deimling M, Huk W (1993) QUEST: a quick echo split NMR imaging technique. Magn Reson Med 29:280–283
17. Hennig J, Hodapp M (1993) Burst imaging. MAGMA 1:39–48
18. Crawley AP, Wood ML, Henkelman RM (1988) Elimination of transverse coherences in FLASH MRI. Magn Reson Med 8:248–60
19. Duerk JL, Lewin JS, Wendt M, Petersilge C (1998) Remember true FISP? A high SNR, near 1-second imaging method for T2-like contrast in interventional MRI at 0.2 T. J Magn Reson Imaging 8:203–208
20. Larson AC, Simonetti OP (2001) Real-time cardiac cine imaging with SPIDER: steady-state projection imaging with dynamic echo-train readout. Magn Reson Med 46:1059–1066
21. Schaeffter T, Weiss S, Holger E, Rasche V (2001) Projection reconstruction balanced fast field echo for interactive real-time cardiac imaging. Magn Reson Med 46:1238–1241
22. Namimoto T, Yamashita Y, Mitsuzaki K, Nakayama Y, Makita O, Kadota M, Takahashi M (2001) Adrenal masses: quantification of fat content with double-echo chemical shift in-phase and opposed-phase FLASH MR images for differentiation of adrenal adenomas. Radiology 218:642–646
23. Nitz WR (1999) MR imaging: acronyms and clinical applications. Eur Radiol 9:979–997
24. Constable RT, Gore JC (1992) The loss of small objects in variable TE imaging: implications for FSE, RARE, and EPI. Magn Reson Med 28:9–24
25. Yuan C, Schmiedl UP, Weinberger E, Krueck WR, Rand SD (1993) Three-dimensional fast spin-echo imaging: pulse sequence and in vivo image evaluation. J Magn Reson Imaging 3:894–899
26. Melhem ER, Itoh R, Folkers PJ (2001) Cervical spine: three-dimensional fast spin-echo MR imaging-improved recovery of longitudinal magnetization with driven equilibrium pulse. Radiology 218:283–288
27. Reimer P, Allkemper T, Schuierer G, Peters PE (1996) Brain imaging: reduced sensitivity of RARE-derived techniques to susceptibility effects. J Comput Assist Tomogr 20:201–205
28. Allkemper T, Reimer P, Schuierer G, Peters PE (1998) Study of susceptibility-induced artefacts in GRASE with different echo train length. Eur Radiol 8:834–838
29. Margosian P, Schmitt F, Purdy D (1986) Faster MR imaging: imaging with half the data. Health Care Instrum 1:195–197
30. Kiefer B, Grässner J, Hausmann R (1994) Image acquisition in a second with half-Fourier acquired single shot turbo spin echo. J Magn Reson Imaging 4:86
31. Parizel PM, Tanghe H, Hofman PAM (1999) Magnetic resonance imaging of the brain. In: Reimer P, Parizel PM, Stichnoth F-A (eds) Clinical MR imaging/a practical approach. Springer, Berlin Heidelberg New York, pp 61–125
32. Hajnal JV, De Coene B, Lewis PD, Baudouin CJ, Cowan FM, Pennock JM, Bydder GM (1992) High signal regions in normal white matter shown by heavily T2-weighted CSF nulled IR sequences. J Comput Assist Tomogr 16:506–513
33. Hashemi RH, Bradley WG Jr, Chen DY, Jordan JE, Queralt JA, Cheng AE, Henrie JN (1995) Suspected multiple sclerosis: MR imaging with a thin-section fast FLAIR pulse sequence. Radiology 196:505–510
34. Palmer S, Bradley WG, Chen DY, Patel S (1999) Subcallosal striations: early findings of multiple sclerosis on sagittal, thin-section, fast FLAIR MR images. Radiology 210:149–153
35. Noguchi N, Ogawa T, Seto H et al. (1997) Subacute and chronic subarachnoid hemorrhage: diagnosis with fluid-attenuated inversion-recovery MR imaging. Radiology 203:257–262
36. Jackson EF, Hayman LA (2000) Meningeal enhancement on fast FLAIR images. Radiology 215:922–924
37. Simonetti OP, Finn JP, White RD, Laub G, Henry DA (1996) "Black blood" T2-weighted inversion-recovery MR imaging of the heart. Radiology 199:49–57
38. Corrado D, Basso C, Thiene G (2000) Arrhythmogenic right ventricular cardiomyopathy: diagnosis, prognosis, and treatment. Heart 83:588–595
39. Barkhausen J, Ruehm SG, Goyen M, Buck T, Laub G, Debatin JF (2001) MR evaluation of ventricular function: true fast imaging with steady-state precession versus fast low-angle shot cine MR imaging: feasibility study. Radiology 219:264–269

40. Shankaranarayanan A, Simonetti O, Laub G, Heid O, Lewin JS, Duerk JL (2001) Real time and segmented True FISP cardiac cine using radial sampling. In: Proc of the 9th Annual Meeting of the ISMRM, Glasgow, p 108
41. Rydberg JN, Lomas DJ, Coakley KJ et al. (1995) Comparison of breath-hold fast spin-echo and conventional spin-echo pulse sequences for T2-weighted MR imaging of liver lesions. Radiology 194:431–437
42. Reimer P, Tombach B (1999) Upper abdomen: liver pancreas, biliary system, and spleen. In: Reimer P, Parizel PM, Stichnoth F-A (eds) Clinical MR imaging/a practical approach. Springer, Berlin Heidelberg New York, pp 247–280
43. Melki PS, Mulkern RV (1992) Magnetization transfer effects in multislice RARE sequences. Magn Reson Med 24:189–195
44. Wolff SD, Balaban RS (1989) Magnetization transfer contrast (MTC) and tissue water proton relaxation in vivo. Magn Reson Med 12:35–37
45. Outwater E, Schnall MD, Braitman LE, Dinsmore BJ, Kressel HY (1992) Magnetization transfer of hepatic lesions: evaluation of a novel contrast technique in the abdomen. Radiology 182:535–540
46. Jeong YY, Mitchell DG, Holland GA (2001) Liver lesion conspicuity: T2-weighted breath-hold fast spin-echo MR imaging before and after gadolinium enhancement: initial experience. Radiology 219:455–460
47. Van Hoe L, Bosmans H, Aerts P, Baert AL, Fevery J, Kiefer B, Marchal G (1996) Focal liver lesions: fast T2-weighted MR imaging with half-Fourier rapid acquisition with relaxation enhancement. Radiology 201:817–823
48. Vitellas KM, Keogan MT, Spritzer CE, Nelson RC (2000) MR cholangiopancreatography of bile and pancreatic duct abnormalities with emphasis on the single-shot fast spin-echo technique. Radiographics 20:939–957
49. Luboldt W, Steiner P, Bauerfeind P, Pelkonen P, Debatin JF (1998) Detection of mass lesions with MR colonography: preliminary report. Radiology 207:59–65
50. Luboldt W, Bauerfeind P, Wildermuth S, Debatin JF (1999) Contrast optimization for assessment of the colonic wall and lumen in MR colonography. J Magn Reson Imaging 9:745–750
51. MacVicar D, Revell P (1999) Pelvis. In: Reimer P, Parizel PM, Stichnoth F-A (eds) Clinical MR imaging/a practical approach. Springer, Berlin Heidelberg New York, pp 299–323
52. Dohke M, Watanabe Y, Okumura A, Amoh Y, Hayashi T, Yoshizako T, Yasui M,Nakashita S, Nakanishi J, Dodo Y (2000) Comprehensive MR imaging of acute gynecologic diseases. Radiographics 20:1551–1566
53. Kurtz AB, Tsimikas JV, Tempany CMC et al. (1999) Diagnosis and staging of ovarian cancer: comparative values of Doppler and conventional US, CT, and MR imaging correlated with surgery and histopathologic analysis: report of the radiology diagnostic oncology group. Radiology 212:19–27
54. Shinmoto H, Kashima K, Yuasa Y, Tanimoto A, Morikawa Y, Ishimoto H, Yoshimura Y, Hiramatsu K (2000) MR imaging of non-CNS fetal abnormalities: a pictorial essay. Radiographics 20:1227–1243
55. Levine D, Barnes PD (1999) Cortical maturation in normal and abnormal fetuses as assessed with prenatal MR imaging. Radiology 210:751–758
56. Jevtic V (2001) Magnetic resonance imaging appearances of different discovertebral lesions. Eur Radiol 11:1123–1135
57. Kreitner KF, Ferber A, Grebe P, Runkel M, Berger S, Thelen M (1999) Injuries of the lateral collateral ligaments of the ankle: assessment with MR imaging. Eur Radiol 9:519–524
58. Uhl M, Ihling Ch, Allmann KH, Laubenberger J, Tauer U, Adler CP, Langer M (1998) Human articular cartilage: in vitro correlation of MRI and histologic findings. Eur Radiol 8:1123–1129
59. Hardy PA, Thomasson D, Recht MP, Piraino D (1996) Optimization of dual echo in the steady state (DESS) free-precession sequence for imaging cartilage. J Magn Reson Imaging 6:329–335
60. Vande Berg BC, Lecouvet FE, Michaux L, Ferrant A, Maldaque B, Malghem J (1998) Magnetic resonance imaging of the bone marrow in hematological malignancies. Eur Radiol 8:1335–1344
61. Vanel D, Bittoun J, Tardivon A (1998) MRI of bone metastases. Eur Radiol 8:1345–1351
62. Chung YC, Merkle EM, Lewin JS, Shonk RJ, Duerk JL (1999) Fast T2-weighted imaging by PSIF at 0.2 T for interventional MRI. Magn Reson Med 42:335–344
63. Quesson B, de Zwart JA, Moonen CTW (2000) Magnetic resonance temperature imaging for guidance of thermotherapy. J Magn Reson Imaging 12:525–533
64. Chung YC, Duerk JL, Shankaranarayanan A, Hampke M, Merkle EM, Lewin JS (1999) Temperature measurement using echo-shifted FLASH at low field for interventional MRI. J Magn Reson Imaging 9:138–145
65. McDannold NJ, King RL, Jolesz FA, Hynynen KH (2000) Usefulness of MR imaging-derived thermometry and dosimetry in determining the threshold for tissue damage induced by thermal surgery in rabbits. Radiology 216:517–523
66. Mueller-Lisse UG, Thoma M, Faber S, Heuck AF, Muschter R, Schneede P, Weninger E, Hofstetter AG, Reiser MF (1999) Coagulative interstitial laser-induced thermotherapy of benign prostatic hyperplasia: online imaging with a T2-weighted fast spin-echo MR sequence: experience in six patients. Radiology 210:373–379
67. Il'yasov KA, Hennig J (1998) Single-shot diffusion-weighted RARE sequence: application for temperature monitoring during hyperthermia session. J Magn Reson Imaging 8:1296–1305
68. Zur Y, Bosak E, Kaplan N (1997) A new diffusion SSFP imaging technique. Magn Reson Med 37:716–722
69. Brockstedt S, Thomsen C, Wirestam R, Holtas S, Stahlberg F (1998) Quantitative diffusion coefficient maps using fast spin-echo MRI. Magn Reson Imaging 16:877–886
70. Barbier EL, Lamalle L, Decorps M (2001) Methodology of brain perfusion imaging. J Magn Reson Imaging 13:496–520
71. Preibisch C, Haase A (2001) Perfusion imaging using spin-labeling methods: contrast-to-noise comparison in functional MRI applications. Magn Reson Med 46:172–182
72. Frahm J, Bruhn H, Merboldt K-D, Hänicke W (1992) Dynamic MR imaging of human brain oxygenation during rest and photic stimulation. J Magn Reson Imaging 2:501–505
73. Duyn JH, Mattay VS, Sexton RH, Sobering GS, Barrios FA, Liu G, Frank JA, Weinberger DR, Moonen CTW (1994) 3-Dimensional functional imaging of human brain using echo-shifted FLASH MRI. Magn Reson Med 32:150–155